HHS Public Access

Author manuscript

Mol Neurobiol. Author manuscript; available in PMC 2016 February 05.

Published in final edited form as:

Mol Neurobiol. 2015 June ; 51(3): 1024–1037. doi:10.1007/s12035-014-8762-1.

Activation of Dopamine D1 Receptors Regulates Dendritic Morphogenesis Through Rac1 and RhoA in Prefrontal Cortex Neurons

Juan Li,
Key Laboratory of Functional Proteomics of Guangdong Province, Department of Pathophysiology, Southern Medical University, Guangzhou 510515, China

Department of Histology and Embryology, Southern Medical University, Guangzhou 510515, China

Jingjing Gu,
Key Laboratory of Functional Proteomics of Guangdong Province, Department of Pathophysiology, Southern Medical University, Guangzhou 510515, China

Bin Wang,
Key Laboratory of Functional Proteomics of Guangdong Province, Department of Pathophysiology, Southern Medical University, Guangzhou 510515, China

Minjuan Xie,
Key Laboratory of Functional Proteomics of Guangdong Province, Department of Pathophysiology, Southern Medical University, Guangzhou 510515, China

Lu Huang,
Key Laboratory of Functional Proteomics of Guangdong Province, Department of Pathophysiology, Southern Medical University, Guangzhou 510515, China

Yutong Liu,
Key Laboratory of Functional Proteomics of Guangdong Province, Department of Pathophysiology, Southern Medical University, Guangzhou 510515, China

Lei Zhang,
Elderly Health Services Research Center, Southern Medical University, Guangzhou 510515, China

Jinhua Xue,
Key Laboratory of Functional Proteomics of Guangdong Province, Department of Pathophysiology, Southern Medical University, Guangzhou 510515, China

Fukun Guo,

✉L. Zhang, Department of Histology and Embryology, Southern Medical University, Guangzhou 510515, China, zlilyzh@126.com.
✉L. Zhang, Department of Pathophysiology, Elderly Health Services Research, Center, Southern Medical University, Guangzhou 510515, China, zlulu70@126.com.
J. Li, J. Gu and B. Wang contributed equally to this work.

Conflict of interest The authors declare no conflict of interest.

Division of Experimental Hematology and Cancer Biology, Children's Hospital Research Foundation, Cincinnati, OH, USA

Lin Zhang, and
Department of Histology and Embryology, Southern Medical University, Guangzhou 510515, China

Lu Zhang
Key Laboratory of Functional Proteomics of Guangdong Province, Department of Pathophysiology, Southern Medical University, Guangzhou 510515, China

Elderly Health Services Research Center, Southern Medical University, Guangzhou 510515, China

Abstract

Dopamine (DA) is an important regulator of neuronal plasticity in the prefrontal cortex (PFC) and plays a critical role in addiction-related neuroadaptation. The Rho GTPases, including Rac1, RhoA and Cdc42, are key regulators of actin cytoskeleton rearrangement that play important roles in dendritic morphogenesis. The goal of the current study was to use cultures of primary PFC neurons to gain a better understanding of the molecular mechanisms underlying DA-induced dendritic morphogenesis, a phenomenon that mimics the increase in DA synaptic transmission observed in the PFC of in vivo cocaine administration. We investigated the effects of repeated DA treatments on dendritic morphology changes in PFC neurons, and identified Rac1 and RhoA as downstream effectors of D1 receptors during the regulation of dendritic morphogenesis. Importantly, we found that D1 receptor-regulated Rac1 and RhoA have distinct roles in the regulation of dendritic morphogenesis after repeated DA treatments. Our data provide the first evidence that Rac1 and RhoA are effectors of D1 receptor signaling during dendritic morphogenesis and represent new signaling molecules involved in long-lasting neuroadaptation in the PFC.

Keywords

D1 receptor; Dendritic cytoskeleton; Prefrontal cortex neurons (PFC); Rac1; RhoA

Introduction

Cocaine produces widespread effects on the structure of neurons throughout the reward system of the brain, and these changes are believed to underlie long-lasting drug-induced behavioral changes [1–3]. For example, repeated exposure to cocaine increases the number of dendrites and the density of spines in brain regions involved in reward, such as the nucleus accumbens (NAc) and the prefrontal cortex (PFC) [4–8]. These changes in dendritic morphology are thought to play key roles in cocaine-induced behavioral plasticity and addiction [9].

Dopamine (DA) receptors of the D1 class (D1 and D5) and the D2 class (D2, D3 and D4) [10, 11] are critically involved in cocaine-induced neurobiological changes [12, 13]. DA, acting on DA receptors, is an important regulator of neuronal morphogenesis in the PFC

[14–16]. This process may play a critical role in producing the effects of DA-releasing stimulants, such as cocaine, on addiction-related neuroadaptation [17, 18]. The main targets of DA terminals in the PFC are pyramidal neurons, and the D1 receptor plays a particularly important role in mediating pyramidal cell morphogenesis after cocaine treatment [14, 19]. Importantly, recent studies have reported that repeated treatment of neurons with DA in vitro may model the effects of repeated cocaine use in vivo [20]. However, the intracellular signaling mechanism that controls this process—particularly the dendritic remodeling—is poorly understood.

Much information has been collected describing dendritic remodeling mechanisms, one of which involves the Rho GTPases. The Rho GTPases, including Rac1, Rho A and Cdc42, are key regulators of actin cytoskeleton rearrangement and play important roles in dendritic morphogenesis [21–25]. It is generally thought that RhoA and Rac1/Cdc42 have antagonistic effects on dendritic spine morphology: Rac1/Cdc42 promotes the development of new spines, whereas RhoA inhibits spine formation and maintenance [26, 27]. Although many studies have illustrated the importance of Rho family GTPases to dendritic morphogenesis, it remains unclear how the activities of these GTPases are appropriately regulated in response to extracellular signaling events during dendritic morphogenesis [28–31].

The goal of the current study was to use primary PFC cultures to gain a better understanding of the molecular mechanism underlying cocaine-induced dendritic morphogenesis. We investigated the effects of repeated DA treatment, mimicking repeated exposure to cocaine, on dendritic morphology changes in PFCs, and we examined the underlying signaling mechanisms. We present evidence that the D1 receptor is critically involved in DA-induced dendritic morphogenesis, and Rac1 and RhoA function as downstream effectors of D1 receptors in the regulation of dendritic morphogenesis. D1 receptor-regulated Rac1 and RhoA have distinct roles in the regulation of dendritic morphogenesis after repeated DA treatment. Additionally, we found evidence of crosstalk between Rac1 and RhoA in the PFC. Our data provide the first evidence that Rac1 and RhoA function downstream of D1 receptor signaling in the PFC to regulate dendritic morphogenesis and that Rac1 and RhoA are thus new signaling molecules involved in long-lasting neuroadaptation in the PFC.

Materials and Methods

Postnatal PFC Cultures

PFC neurons were isolated as described previously [16, 20]. Briefly, postnatal day 1 SD rats were sacrificed by decapitation. The PFC was dissected and dissociated with 0.125 % trypsin at 37 °C for 10 min. The cells were plated onto coverslips coated with poly-D-lysine (100 μg/ml; Sigma, St. Louis, MO, USA) in 24-well culture plates at a density of 20,000 cells/plate. The cells were planted in DMEM/F12 supplemented with penicillin (100 U/ml) and streptomycin (100 U/ml); after 4 h had elapsed, the medium was replaced with neurobasal medium (Gibco, Auckland, New Zealand) supplemented with 2 % B27 (Gibco) and 0.5 mM glutamine with 0.5 μM AraC added at 2 days in vitro (DIV). The neurons were cultured for an additional 5 days before infection and/or treated with various reagents, as specified.

Drug Treatments

PFC neurons were treated with either phosphate-buffered saline (PBS), DA (1 μM, 30 min) or SKF81297 (1 μM, 15 min) on days 11, 13 and 15 in culture, cells were collected 4 days after repeated treatment (day 19) as previously reported [20]. The D1 receptor antagonist SCH23390 (10 μM) was added 5 min before DA stimulation. The Rac1-specific inhibitor NSC23766 (100 μM) and a specific inhibitor of Rock (which functions downstream of RhoA), Y27632 (100 μM), were added 3 min before DA stimulation.

Virus Production and Infection of PFC Neurons

For lentivirus expression, cDNAs encoding the dominant-negative mutants Rac1 (Rac1N17) and RhoA (RhoAN19) and the active mutants Rac1 (Rac1L61) and RhoA (RhoAL63) were ligated into the *Bam*HI and *Xho*I sites of the lentiviral vector Plenti6/V5-topo, which expresses enhanced green fluorescent protein (EGFP) bicistronically [32, 33]. Recombinant lentiviruses were produced using the ViralPower Lentiviral Expression System (Invitrogen). The virus was concentrated 10–15× by centrifugation using a Centricon plus-020 filter (Millipore) following the manufacturer's instructions. Aliquots were stored at −80 °C. All virus preparations were titered according to the ViralPower protocol and were verified to contain approximately 5×10^8 infectious units/μl. Viral infection was performed by incubating lentiviruses with PFC neurons at DIV7, and the cells were grown for 12 days before fixation.

Analysis of Rac1 and RhoA GTPase Activity

G-Lisa™ RhoA or Rac1 luminescence-based Biochem kits (Cytoskeleton, Denver, CO, USA) were used for the small GTPase activation assays. All procedures were performed by strictly following the manufacturer's instructions. Briefly, cells were grown in a 35-mmdish, transfected when indicated, and treated with DA/antagonist on DIV 11, 13, and 15 in culture, then lysed in the provided lysis buffer (including protease inhibitors) at 0 (PBS), 10, 40, 60, 120 min following the last treatment. After correction of the total protein concentration, half of the extract volume (40 μl) was mixed with the provided binding buffer, added to the G-Lisa™ plates and incubated on ice for 30 min. The wells were washed, and active GTPase was detected by specific antibodies in a luminescent reaction measured in a BioTek Epoch™ Ultramicro Spectrophotometer according to the manufacturer's instructions. In parallel, an aliquot from each supernatant extract was analyzed by western blotting to determine endogenous RhoA and Rac1 levels and confirm comparable total protein content between the samples.

Dendrite and Spine Imaging and Analysis

The cultures were incubated with a mouse monoclonal antibody against MAP2 (1:1,000) (Chemicon International, Temecula, CA, USA) [34, 35] to visualize dendrites or a sheep antibody against γ-actin (1:1,000) (Chemicon International) to visualize spines. Primary antibodies were detected with anti-mouse Alexa Fluor 546 or anti-sheep Alexa Fluor 488 (1:600) secondary antibodies (Molecular Probes, Invitrogen, Carlsbad, CA, USA). For this study, we defined spines, acquired using Zeiss LSM710 confocal (Zeiss, Germany), as being less than 3 μm in length [36], the spines have constricted necks, with heads exceeding 0.6

μm in diameter are defined as mushroom spine, or thin spine with smaller heads, other spines are stubby spine with head widths equal to neck lengths [37–40]. To determine the density of dendritic spines, we measured the lengths of all dendrites of a given neuron and manually counted the spines (provided that they clearly emanated from the dendrites of that particular neuron) to calculate the number per 10 μm. The dendritic complexity was calculated using a Sholl analysis of ring intersections [4, 41]. For each experimental group, cells from at least three different wells were used, and approximately eight cells from each well were analyzed. The images were acquired using Image Pro Plus version 5.1 (Media Cybernetics, Silver Spring, MD, USA). Dendrites and spines were compared using a one-way ANOVA followed by a Bonferroni post-hoc test. Significance levels were set at $p<0.05$.

Synaptic Colocalization Imaging and Analysis

On the 19th day of culture, the culture medium was removed carefully and the neurons were washed once with PBS. The neuron cultures were then fixed with freshly prepared 4 % paraformaldehyde and 4 % sucrose in 0.1 M PBS for 30 min. The fixative was pre-warmed to 37 °C and allowed to cool to room temperature during the fixation period. Then, the fixed cells were permeabilized at room temperature (RT) for 15 min with 0.2 % Triton X-100 in PBS, blocked in PBS with 1 % BSA for 60 min, and incubated with a monoclonal antibody (all antibodies were diluted 1:100 in 0.4 % Triton X-100 and 1 % BSA) overnight at 4 °C followed by the addition of a biotin-conjugated secondary antibody for 1 h at room temperature. The primary antibodies used included a rabbit monoclonal antibody to Synapsin-I, a mouse monoclonal antibody to post-synaptic density protein (PSD-95) (both from Millipore). The cognate secondary antibodies included donkey anti-rabbit IgG (green), and fluorophore-labeled goat antimouse (red). The neurons were imaged using a 40× immersion objective on a Zeiss Axioplan microscope (Zeiss Inc., Oberkochen, Germany). Digital images were acquired with a CCD camera. All images were acquired with AxioUS40V software. For each experimental group, cells from at least three different wells were used, and approximately eight cells from each well were analyzed. All images were acquired using Image Pro Plus version 5.1 (Media Cybernetics). Synapse densities were compared using a one-way ANOVA followed by a Bonferroni post-hoc test. Significance levels were set at $p<0.05$.

Results

Repeated DA Treatment Induces the Structural Morphogenesis of Dendrites and Spines in PFCs

Repeated exposure to cocaine induces dendritic rearrangement in brain areas, including the PFC, that play critical roles in addiction-related neuroadaptation. Sun et al. recently developed an effective in vitro model system by repeatedly treating cultured neurons with low concentrations of DA to mimic the effects of repeated in vivo cocaine exposure. This system was used to demonstrate that repeated DA treatment can reproduce some key aspects of cocaine-related functional changes, thus indicating that this in vitro model system for studying DA-induced neuroadaptation is useful for the investigation of cocaine-induced neuroadaptation [20]. In the current study, we first investigated whether repeated DA treatment can induce morphogenesis in PFC neurons. PFC neurons were treated with either

vehicle or DA (1 μM, 30 min) on days 11, 13 and 15 of culture. Four days after intermittent DA treatment, the cells were analyzed to determine the presence of structural morphogenesis of dendrites and spines. To detect dendritic branching and spine density, the cells were immunostained for MAP2 to highlight the dendritic arbor, and the cells were immunostained for γ-actin to highlight actin-based filopodia and spines [36]. As shown in Fig. 1a, b, d, and e, compared with PBS treatment, repeated DA treatment led to increases in dendritic branching (61.83 % increase, 24±2.374 vs. 14.83±1.794, $p<0.001$, $n=24$ neurons) and spine density (19.66 % increase, 9.19±0.36 vs. 6.68±0.32, $p<0.001$, $n=24$ neurons) in PFC neurons.

To evaluate the number of synapses on a dendrite, the cells were double stained for the post-synaptic marker PSD-95 and the pre-synaptic marker synapsin I. A synapse was defined as a site where PSD-95 and synapsin I puncta overlapped [30, 31]. As shown in Fig. 1c and f, compared with PBS treatment, repeated DA treatment led to an increase in the number of synapses (53.44 % increase, 4.68±0.70 vs. 3.05±0.28, $p<0.001$) in PFC neurons.

BDNF, a potent modulator of synaptic plasticity in the CNS [42–44], has been shown to be capable of increasing spine density and dendritic branching in several different brain areas [44–46]. Therefore, we used BDNF treatment as a positive control. We found that dendritic reorganization induced by a low concentration of DA was similar to BDNF-induced dendritic morphogenesis based on morphological criteria (68.0 % increase in dendrite branching, 24.92±1.93 vs. 14.83±1.79, $p<0.001$; 19.27 % increase in spine density, 9.16±0.25 vs. 6.68±0.32, $p<0.001$; 53.11 % increase in synapse number, 4.67±0.55 vs. 3.05±0.28, $p<0.001$, $n=24$ neurons) (Fig. 1a–e).

As a complementary measurement of dendritic complexity, we performed a standard Sholl analysis, which counts the number of dendritic intersections with concentric circles centering on the cell soma and spaced 20 μm apart. As shown in Fig. 1g, we observed an increased dendritic complexity following repeated DA treatment compared to PBS-treated neurons. Meanwhile, BDNF treatment also increased the number of dendritic intersections compared to PBS-treated neurons. Taken together, these data suggest that repeated DA treatment induces the structural morphogenesis of dendrites and spines in PFCs.

The DA-Induced Structural Morphogenesis of Dendrites and Spines in PFC Neurons Is Regulated by D1 Receptors

DA D1 receptors play important roles in the regulation of cocaine-induced neuroadaptation [47–50]. In support of this, we found that SKF81297, an agonist of the D1 receptor, induced an increase in dendritic branching, spine density and synapse number of PFC neurons (Fig. 2a–f). Sholl analysis also revealed that SKF81297 treatment increased the number of dendritic intersections of the neurons compared to PBS-treated neurons (Fig. 2g). To determine whether DA-induced changes in dendritic morphology are regulated by the D1 receptor, we used a D1 receptor inhibitor, SCH23390, to block D1 receptor function. As shown in Fig. 2a–f, pretreatment of neurons with SCH23390 blocked the effects of chronic DA treatment on dendrite number (54.5 % decrease, 10.92±1.17 vs. 24±2.37, $p<0.001$), spine density (27.31% decrease, 5.68±0.25 vs. 9.19±0.36, $p<0.001$) and synapse number (54.70 % decrease, 2.12±0.61 vs. 4.68±0.70, $p<0.001$) in PFC neurons. By Sholl analysis,

we found that repeated DA treatment induced increasing dendritic intersections, whereas this increase was abolished by pretreatment of neurons with SCH23390 (Fig. 2g). Collectively, these data suggest that the DA-induced structural morphogenesis of dendrites and spines in PFC neurons is regulated by D1 receptors.

Expression of Mutant Rho GTPase in PFCs

To examine the role of Rho GTPase in dendritic morphogenesis, we first generated lentiviruses bearing fusion proteins of green fluorescent protein (GFP) with dominant-negative (DN) Rac1 (Rac1N17) or RhoA (RhoAN19) or constitutively active (CA) Rac1 (Rac1L61) or RhoA (RhoAL63). Expression of the GTPase-GFP mutants was confirmed by immunofluorescence staining. Immunofluorescence staining with antibodies against GFP and MAP2 demonstrated that these recombinant viruses consistently infected >95 % of the neurons (Fig. 3a and b). The effects of expressing Rac1N17, Rac1L61, RhoAN19 or RhoAL63 on the number of dendrites and the spine density of PFCs were examined. We found that expression of Rac1L61 resulted in a slight but significant increase in the number of dendrites and in the spine density, whereas expression of Rac1N17 did not affect these parameters. Expression of RhoAN19 slightly increased the number of dendrites and the spine density, whereas expression of RhoAL63 decreased these parameters (Fig. 3c). These data are consistent with previous findings indicating that Rac1 promotes spine formation, whereas RhoA inhibits it [25].

Regulation of Rho GTPase Activity by DA in PFC Neurons

To determine whether DA regulates Rho GTPase activity, we treated PFC neurons with DA (1 μM) at different time points on DIV 11, 13 and 15, and carried out luminescence-based biochemical assays. We observed a marked activation of Rac1 within 10 min after application of DA, with a maximal effect observed at 40 min, whereas RhoA activity was downregulated 10 min after application of DA (Fig. 4a and b). The data presented in Fig. 4a and b illustrate that repeated DA treatment concurrently upregulates Rac1 activity and downregulates RhoA activity in the PFC. To further probe the interaction between Rac1 and RhoA after DA treatment in the PFC, we analyzed RhoA activity under different conditions. As shown in Fig. 4c, DA treatment caused a 45 % reduction in RhoA activity compared with the control at the 40 min time point. Infection of Rac1L61 for 3 h also caused a 36.4% reduction in RhoA activity, and when DA was added, RhoA activity was not further reduced. On the contrary, when the PFC was infected with Rac1N17, RhoA activity was significantly increased, and expression of Rac1N17 inhibited the DA-mediated downregulation of RhoA activity. These data indicate that Rac1 interacts with RhoA in the PFC and that Rac1 activity is necessary for the DA-mediated downregulation of RhoA activity.

Rac1 Mediates DA-Induced Structural Morphogenesis of Dendrites and Spines in PFCs

Because Rac1 has been reported to contribute to spine formation, we next investigated the function of Rac1 in the regulation of DA-induced structural morphogenesis in PFCs. PFC neurons at DIV7 were infected with Rac1N17 or Rac1L61 lentivirus and treated with either vehicle (EGFP) or DA (1 μM, 30 min) on days 11, 13 and 15 of culture. Four days after intermittent DA treatment, the cells were analyzed to determine the structural

morphogenesis of dendrites and spines. We found that expression of Rac1N17 abolished the DA-induced increases in dendrites (55.54% decrease, 10.67±1.23 vs. 24±2.37) and spine density (29.27% decrease, 6.50±0.19 vs. 9.19±0.36, $p<0.001$), whereas expression of Rac1L61 enhanced the DA-induced increase in dendrites (23.25 % increase, 29.58±1.28 vs. 24±2.37, $p<0.001$) and spine density (21.55 % increase, 11.17±0.43 vs. 9.19±0.36, $p<0.05$) (Fig. 5a, b, d, and e). Similarly, expression of Rac1N17 abated the DA-induced increase in synapse number (55.13 % decrease, 2.1±0.43 vs. 4.68±0.70, $p<0.001$), whereas expression of Rac1L61 enhanced the DA-induced increase in synapse number (25.43 % increase, 5.87±0.61 vs. 4.68±0.70, $p<0.001$) (Fig. 5c and f). Meanwhile, we found that NSC23766, a structure-based, reversible, Rac1-specific inhibitor that blocks Rac1 but not RhoA or Cdc42 activation [51] inhibited the DA-induced increase in dendrites (54.67 % decrease, 10.88±1.31 vs. 24±2.37, $p<0.001$), spine density (27.09 % decrease, 6.7±0.27 vs. 9.19±0.36, $p<0.001$) and synapse number (56.62% decrease, 2.03±0.30 vs. 4.68±0.70, $p<0.001$). In addition, Sholl analysis shown in Fig. 5g indicated an increased dendritic complexity following repeated DA treatment compared to PBS-treated neurons. Interestingly, pretreatment of neurons with Rac1L61 further increased the number of dendritic intersections of the neurons compared to DA-treated neurons. In contrast, pretreatment of neurons with NSC23766 or Rac1N17 decreased the number of dendritic intersections compared to DA-treated neurons. These observations indicate that the activation of Rac1 following DA stimulation mediates the structural morphogenesis of dendrites and spines in PFC neurons.

RhoA Signaling Is Involved in the DA-Induced Structural Morphogenesis of Dendrites and Spines in PFC Neurons

We next focused on the effect of RhoA on the DA-induced structural morphogenesis of dendrites and spines in PFC neurons. PFC neurons were infected with RhoAN19 or RhoAL63 lentiviruses. We observed that expression of RhoAN19 enhanced the DA-induced increase in dendrites (21.88 % increase, 29.25±1.38 vs. 24±2.37, $p<0.001$) and spine density (24.59 % increase, 11.45±0.22 vs. 9.19±0.36, $p<0.05$), whereas expression of RhoAL63 abated the DA-induced increase in dendrites (51.04 % decrease, 11.75±1.77 vs. 24±2.37, $p<0.001$) and spine density (21.55 % decrease, 7.21±0.30 vs. 9.19±0.36, $p<0.001$) (Fig. 6a, b, d and e). In addition, the expression of RhoAN19 enhanced the DA-induced increase in synapse number (32.05 % increase, 6.18±0.79 vs. 4.68±0.70, $p<0.05$), whereas expression of RhoAL63 reduced the DA-induced increase in synapse number (55.56 % decrease, 2.08±0.27 vs. 4.68±0.70, $p<0.001$) (Fig. 6c and f). Sholl analysis shown in Fig. 6g indicated that pretreatment of neurons with RhoAN19 further increased the number of dendritic intersections of the neurons compared to DA-treated neurons. In contrast, pretreatment of neurons with RhoAL63 decreased the number of dendritic intersections compared to DA-treated neurons. Thus, RhoA plays a role in DA-induced structural morphogenesis of dendrites and spines in PFC neurons.

RhoA acts via different effectors, including Rho kinase (ROCK), to regulate diverse cellular functions. To determine the means by which RhoA regulates DA-induced dendritic morphogenesis, we analyzed the involvement of ROCK. We treated PFC neurons with Y-27632 (100 μM), a specific inhibitor of ROCK, prior to each DA treatment and analyzed

the structural morphogenesis of dendrites and spines in PFC neurons. The number of dendrites (24.75±1.96), spine density (9.08±0.24) and synapse number (4.93±0.62) were not obviously affected (Fig. 6a–f), suggesting that DA might activate a RhoA-dependent but ROCK-independent signaling pathway to stimulate the structural morphogenesis of dendrites and spines in PFC neurons.

The Involvement of Rac1 and RhoA in the DA-Induced Structural Morphogenesis of Dendrites and Spines Is Mediated by the D1 Receptor

To determine whether the involvement of Rac1 and RhoA in the DA-induced structural morphogenesis of dendrites and spines is mediated by the D1 receptor, we first performed biochemical assays to analyze the effect of SCH23390 on the DA-induced changes in Rac1 and RhoA activity. We found that SCH23390 inhibited the DA-induced changes in Rac1 and RhoA activity, indicating that DA signals through the D1 receptor to induce changes in Rac1 and RhoA activity (Fig. 7a). Next, we sought to determine whether Rac1 and RhoA function downstream of the D1 receptor to regulate dendritic morphogenesis. For these experiments, we used the SKF81297-treated model as described previously [52]. PFC neurons were treated with PBS or the D1-like agonist SKF81297 on DIV 11, 13 and 15. Four days after treatment, the dendrites and dendritic spines were analyzed. As shown in Fig. 7b–g, compared with PBS treatment, SKF81297 treatment led to an increase in dendritic branching (74.78 % increase, 25.92±1.28 vs. 14.83±1.79, $p<0.001$), spine density (17.71 % increase, 9.04±0.25 vs. 7.68±0.32, $p<0.001$) and synapse number (61.64 % increase, 4.93±0.65 vs. 3.05±0.28, $p<0.001$) in cultured PFC neurons. Importantly, we observed that expression of Rac1N17 abated the SKF-induced increase in dendrites (57.56 % decrease, 11±1.54 vs. 25.92±1.28, $p<0.001$), spine density (27.77 % decrease, 6.53±0.19 vs. 9.04±0.24, $p<0.001$) and synapse number (28.40 % decrease, 3.53±0.48 vs. 4.93±0.65, $p<0.001$), whereas expression of Rac1L61 enhanced the SKF-induced increase in dendrites (24.42 % increase, 32.25±1.31 vs. 25.92±1.28, $p<0.001$), spine density (24.00 % increase, 11.21±0.41 vs. 9.04±0.24, $p<0.05$) and synapse number (36.11 % increase, 6.71±0.58 vs. 4.93±0.65, $p<0.001$) (Fig. 7b–g). In addition, the expression of RhoAN19 enhanced the SKF-induced increase in dendrites (20.87 % increase, 31.33 ± 1.53 vs. 25.92 ± 1.28, $p<0.05$), spine density (28.32 % increase, 11.60±0.29 vs. 9.04±0.24, $p<0.05$) and synapse number (38.54 % increase, 6.83±0.96 vs. 4.93±0.65, $p<0.001$), whereas expression of RhoAL63 abated the SKF-induced increase in dendrites (55.63 % decrease, 11.5±1.57 vs. 25.92±1.28, $p<0.001$), spine density (22.90 % decrease, 6.97±0.32 vs. 9.04±0.24, $p<0.001$) and synapse number (32.66 % decrease, 3.32±0.46 vs. 4.93±0.65, $p<0.001$) (Fig. 7b–g). In addition, Sholl analysis shown in Fig. 7h indicated an increased dendritic complexity following repeated SKF81297 treatment compared to PBS-treated neurons. Pretreatment of neurons with Rac1L61 or RhoAN19 further increased the number of dendritic intersections of the neurons compared to SKF-treated neurons. In contrast, pretreatment of neurons with Rac1N17 or RhoAL63 decreased the number of dendritic intersections compared to SKF-treated neurons. These results indicate that the regulation of dendritic morphogenesis may be mediated via Rac1 and RhoA signaling through the D1 receptor.

To further determine which spine subtype is changed, spine type analysis was carried out according to the published methods [37–40]. Dendritic spines were classified into three

types, including mushroom spines (spines with constricted necks and heads exceeding 0.6 μm in diameter), thin spines (spines that have constricted necks and small heads), and stubby spines (spines that have head widths equal to the neck length). We found that, compared with PBS treatment, repeated DA treatment led to an increase in thin spine density, not of stubby and mushroom spines. Similar results were found in BDNF or SKF81297 treatment group. Meanwhile, we observed that SCH23390 pretreatment decreased all three type spine density, while RhoAN19 and Rac1L61 pretreatment led to increase of all three type spine, but RhoAL63, Rac1N17, and NSC23766 pretreatment only led to the decrease of thin spine density. Similarly, compared with SKF81297 treatment, RhoAN19 and Rac1L61 pretreatment also led to the increase of all three type spine density, but RhoAL63 and Rac1N17 pretreatment only led to the decrease of thin spine density (Fig. 8a, b, c).

Discussion

Dendritic remodeling in the adult brain has been strongly implicated in the neuroadaptation that underlies several psychiatric diseases, including cocaine addiction [3, 43]. Similarly, it has recently become clear that the structural plasticity of dendritic spines is associated with synaptic plasticity [53, 54]. In the current study, using the PFC model with repeated DA treatment, we present evidence that DA D1 receptors regulate dendritic morphogenesis through Rac1 and RhoA.

The DA D1 receptor is widely expressed in brain areas involved in reward, including the PFC, and plays a critical role in mediating the cellular and behavioral effects of cocaine [13, 47, 52, 55]. Repeated cocaine exposure causes an increase in DA concentration, resulting in long-lasting dendritic morphology changes in brain reward areas, such as the PFC [17, 56]. DA is one of the most important regulators of neuronal plasticity in addiction-related neuroadaptation [14, 57–59]. In the PFC, the main targets of DA terminals are pyramidal neurons. Sun et al. recently developed an effective in vitro model system by repeatedly treating cultured neurons with low concentrations of DA to mimic the effects of repeated in vivo cocaine exposure [20]. These authors showed that repeated DA treatment can reproduce some key aspects of cocaine-related functional changes, thus indicating that their in vitro model system for studying DA-induced neuroadaptation is useful for investigating cocaine-induced neuroadaptation [20]. We first set up a similar PFC model with repeated DA treatment, and we found that repeated DA treatment induced the structural morphogenesis of dendrites and spines in PFCs, which is very similar to the effect of cocaine in vivo. Next, we found that pretreatment of PFC neurons with a D1 receptor inhibitor impaired the ability of DA to induce dendritic morphogenesis. Together with our previous data indicating that treatment with SKF81297, an agonist of the D1 receptor, led to an increase in the dendritic branching and spine density of PFC neurons [52, 60], the current data suggest that the DA-induced structural morphogenesis of the dendrites and spines of PFC neurons is regulated by the D1 receptor.

Dendritic remodeling requires architectural changes in dendrites and spines through modification of the actin cytoskeleton [61]. Previous studies have indicated that changes in spine morphology are controlled by modifications of the actin cytoskeleton that are regulated by small GTPases [18, 22, 48]. The Rho family of small GTPases, including Rac1,

RhoA and Cdc42, are key regulators of actin cytoskeleton rearrangement and play important roles in dendritic morphogenesis [21, 48]. We observed marked activation of Rac1 within 10 min after application of DA, whereas RhoA activity was downregulated 10 min after application of DA. Importantly, we found evidence for crosstalk between Rac1 and RhoA in PFC neurons. The expression of Rac1L61 and treatment with DA decreased RhoA activity to a similar extent; however, the effects of Rac1L61 and DA on RhoA activity were not additive. On the other hand, Rac1N17 elevated RhoA activity and inhibited the reduction of RhoA activity that follows DA treatment. These data indicate the complexity of Rho GTPase regulation in dendritic morphogenesis. We have also provided evidence that Rac1 and RhoA are both involved in mediating DA-induced structural morphogenesis in PFCs, and Rac1 and RhoA have distinct functions in the regulation of dendritic morphogenesis after repeated DA treatment.

We tested the hypothesis that Rac1 and RhoA function with the D1 receptor to regulate dendritic morphogenesis after repeated DA treatment. Consistent with this idea, we found that inhibition of D1 receptor function with SCH23390 inhibited the increase in Rac1 activity and the decrease in RhoA activity observed after DA treatment. Meanwhile, we found that expression of a dominant negative Rac1 decreased the SKF-induced increase in dendrites, spine density and synapse number, whereas expression of a CA Rac1 increased the SKF-induced increase in dendrites, spine density and synapse number. Conversely, the expression of dominant negative RhoA enhanced the SKF-induced increase in dendrites, spine density and synapse number, whereas expression of CA RhoA reduced the SKF-induced increase in dendrites, spine density and synapse number. These results indicate that the regulation of dendritic morphogenesis by the D1 receptor may be mediated via Rac1 and RhoA signaling.

In summary, these findings support the hypothesis that the D1 receptor is necessary and sufficient for mediating DA-induced dendritic morphogenesis (Fig. 8d). Furthermore, regulation of dendritic morphogenesis by the D1 receptor involves the modulation of Rac1 and RhoA activity. In addition, we have provided evidence of crosstalk between Rac1 and RhoA in PFC neurons after DA treatment. These findings suggest a signaling mechanism in which Rac1 and RhoA, regulated by the D1 receptor, differentially modulate dendritic morphogenesis in PFC neurons after DA treatment. These data provide fundamental insights into the signaling pathways controlling cocaine-induced structural morphogenesis, which has been implicated in the persistence of drug addiction.

Acknowledgments

This work is supported by the Natural Science Foundation of China (81171824, 81371719 and 81371509), Foundation for High-level Talents in Higher Education of Guangdong(C1031118, C2050205), the Key Project of the Chinese Ministry of Education (21132), Major Breakthroughs in Key Areas and Projects of Guangdong and Hongkong (2011A011304001), Science and Technology Program of Guangzhou (12C32121608, 201300000183), Major cooperation project of the science and Technology of Guangdong Province (2011A090100025) and Research Fund for the Doctoral Program of Higher Education of China (201334433110017).

References

1. Thomas MJ, Kalivas PW, Shaham Y. Neuroplasticity in the mesolimbic dopamine system and cocaine addiction. Br J Pharmacol. 2008; 154(2):327–342. [PubMed: 18345022]

2. Robinson TE, Grazyna G, Mitton E, Kolb B. Cocaine self-administration alters the morphology of dendrites and dendritic spines in the nucleus accumbens and neocortex. Synapse. 2001; 39(3):257–266. [PubMed: 11169774]

3. Luscher C, Bellone C. Cocaine-evoked synaptic plasticity: a key to addiction? Nat Neurosci. 2008; 11(7):737–738. [PubMed: 18575469]

4. Robinson TE, Kolb B. Alterations in the morphology of dendrites and dendritic spines in the nucleus accumbens and prefrontal cortex following repeated treatment with amphetamine or cocaine. Eur J Neurosci. 1999; 11(5):1598–1604. [PubMed: 10215912]

5. Robinson TE, Gorny G, Mitton E, Kolb B. Cocaine self-administration alters the morphology of dendrites and dendritic spines in the nucleus accumbens and neocortex. Synapse. 2001; 39(3):257–266. [PubMed: 11169774]

6. Norrholm SD, Bibb JA, Nestler EJ, Ouimet CC, Taylor JR, Greengard P. Cocaine-induced proliferation of dendritic spines in nucleus accumbens is dependent on the activity of cyclin-dependent kinase-5. Neuroscience. 2003; 116(1):19–22. [PubMed: 12535933]

7. Russo SJ, Wilkinson MB, Mazei-Robison MS, Dietz DM, Maze I, Krishnan V, Renthal W, Graham A, Birnbaum SG, Green TA, Robison B, Lesselyong A, Perrotti LI, Bolanos CA, Kumar A, Clark MS, Neumaier JF, Neve RL, Bhakar AL, Barker PA, Nestler EJ. Nuclear factor kappa B signaling regulates neuronal morphology and cocaine reward. J Neurosci. 2009; 29(11):3529–3537. [PubMed: 19295158]

8. Lee HK, Kirkwood A. AMPA receptor regulation during synaptic plasticity in hippocampus and neocortex. Semin Cell Dev Biol. 2011; 22(5):514–520. [PubMed: 21856433]

9. Robinson TE, Kolb B. Morphine alters the structure of neurons in the nucleus accumbens and neocortex of rats. Synapse. 1999; 33(2):160–162. [PubMed: 10400894]

10. Gerfen C, Engber T, Mahan L, Susel Z, Chase T, Monsma F, Sibley D. D1 and D2 dopamine receptor-regulated gene expression of striatonigral and striatopallidal neurons. Science. 1990; 250(4986):1429–1432. [PubMed: 2147780]

11. Civelli O, Bunzow JR, Grandy DK. Molecular diversity of the dopamine receptors. Annu Rev Pharmacol Toxicol. 1993; 33:281–307. [PubMed: 8494342]

12. Surmeier DJ, Ding J, Day M, Wang Z, Shen W. D1 and D2 dopamine-receptor modulation of striatal glutamatergic signaling in striatal medium spiny neurons. Trends Neurosci. 2007; 30(5): 228–235. [PubMed: 17408758]

13. Liu NY, Zhang L, Wang XN. Mediating effect of dopamine D3 receptors on Jak2 and GABAAalpha1 expression in mouse brains induced by cocaine. Chin Med J. 2007; 120(10):910–914. [PubMed: 17543182]

14. Sun X, Zhao Y, Wolf ME. Dopamine receptor stimulation modulates AMPA receptor synaptic insertion in prefrontal cortex neurons. J Neurosci. 2005; 25(32):7342–7351. [PubMed: 16093384]

15. Castner SA, Williams GV. Tuning the engine of cognition: a focus on NMDA/D1 receptor interactions in prefrontal cortex. Brain Cogn. 2007; 63(2):94–122. [PubMed: 17204357]

16. Gao C, Wolf ME. Dopamine receptors regulate NMDA receptor surface expression in prefrontal cortex neurons. J Neurochem. 2008; 106(6):2489–2501. [PubMed: 18673451]

17. Kauer JA, Malenka RC. Synaptic plasticity and addiction. Nat Rev Neurosci. 2007; 8(11):844–858. [PubMed: 17948030]

18. Beninger R, Banasikowski T. Dopaminergic mechanism of reward-related incentive learning: focus on the dopamine d3 receptor. Neurotox Res. 2008; 14(1):57–69. [PubMed: 18790725]

19. Campana AD, Sanchez F, Gamboa C, Gomez-Villalobos MJ, De La Cruz F, Zamudio S, Flores G. Dendritic morphology on neurons from prefrontal cortex, hippocampus, and nucleus accumbens is altered in adult male mice exposed to repeated low dose of malathion. Synapse. 2008; 62(4):283–290. [PubMed: 18240323]

20. Sun X, Milovanovic M, Zhao Y, Wolf ME. Acute and chronic dopamine receptor stimulation modulates AMPA receptor trafficking in nucleus accumbens neurons cocultured with prefrontal cortex neurons. J Neurosci. 2008; 28(16):4216–4230. [PubMed: 18417701]

21. Dietz DM, Sun H, Lobo MK, Cahill ME, Chadwick B, Gao V, Koo JW, Mazei-Robison MS, Dias C, Maze I, Damez-Werno D, Dietz KC, Scobie KN, Ferguson D, Christoffel D, Ohnishi Y, Hodes GE, Zheng Y, Neve RL, Hahn KM, Russo SJ, Nestler EJ. Rac1 is essential in cocaine-induced

structural plasticity of nucleus accumbens neurons. Nat Neurosci. 2012; 15(6):891–896. [PubMed: 22522400]

22. Threadgill R, Bobb K, Ghosh A. Regulation of dendritic growth and remodeling by Rho, Rac, and Cdc42. Neuron. 1997; 19(3):625–634. [PubMed: 9331353]
23. Tashiro A, Yuste R. Regulation of dendritic spine motility and stability by Rac1 and Rho kinase: evidence for two forms of spine motility. Mol Cell Neurosci. 2004; 26(3):429–440. [PubMed: 15234347]
24. Ng J, Luo L. Rho GTPases regulate axon growth through convergent and divergent signaling pathways. Neuron. 2004; 44(5):779–793. [PubMed: 15572110]
25. Ng J, Nardine T, Harms M, Tzu J, Goldstein A, Sun Y, Dietzl G, Dickson BJ, Luo L. Rac GTPases control axon growth, guidance and branching. Nature. 2002; 416(6879):442–447. [PubMed: 11919635]
26. Tashiro A, Minden A, Yuste R. Regulation of dendritic spine morphology by the Rho family of small GTPases: antagonistic roles of Rac and Rho. Cereb Cortex. 2000; 10(10):927–938. [PubMed: 11007543]
27. Nakayama AY, Luo L. Intracellular signaling pathways that regulate dendritic spine morphogenesis. Hippocampus. 2000; 10(5):582–586. [PubMed: 11075828]
28. Auer M, Hausott B, Klimaschewski L. Rho GTPases as regulators of morphological neuroplasticity. Ann Anat. 2011; 193(4):259–266. [PubMed: 21459565]
29. Martino A, Ettorre M, Musilli M, Lorenzetto E, Buffelli M, Diana G. Rho GTPase-dependent plasticity of dendritic spines in the adult brain. Front Cell Neurosci. 2013; 7:62. [PubMed: 23734098]
30. Vadodaria KC, Brakebusch C, Suter U, Jessberger S. Stage-specific functions of the small Rho GTPases Cdc42 and Rac1 for adult hippocampal neurogenesis. J Neurosci. 2013; 33(3):1179–1189. [PubMed: 23325254]
31. Nakagawa H, Miki H, Ito M, Ohashi K, Takenawa T, Miyamoto S. N-WASP, WAVE and Mena play different roles in the organization of actin cytoskeleton in lamellipodia. J Cell Sci. 2001; 114(8):1555–1565. [PubMed: 11282031]
32. Guo F, Zheng Y. Rho family GTPases cooperate with p53 deletion to promote primary mouse embryonic fibroblast cell invasion. Oncogene. 2004; 23(33):5577–5585. [PubMed: 15122327]
33. Guo F, Zheng Y. Involvement of Rho family GTPases in p19Arf- and p53-mediated proliferation of primary mouse embryonic fibroblasts. Mol Cell Biol. 2004; 24(3):1426–1438. [PubMed: 14729984]
34. Ito D, Tamate H, Nagayama M, Uchida T, Kudoh SN, Gohara K. Minimum neuron density for synchronized bursts in a rat cortical culture on multi-electrode arrays. Neuroscience. 2010; 171(1):50–61. [PubMed: 20800660]
35. Ghiretti AE, Paradis S. The GTPase Rem2 regulates synapse development and dendritic morphology. Dev Neurobiol. 2011; 71(5):374–389. [PubMed: 21485012]
36. McCroskery S, Bailey A, Lin L, Daniels MP. Transmembrane agrin regulates dendritic filopodia and synapse formation in mature hippocampal neuron cultures. Neuroscience. 2009; 163(1):168–179. [PubMed: 19524020]
37. Bourne JN, Harris KM. Balancing structure and function at hippocampal dendritic spines. Annu Rev Neurosci. 2008; 31:47–67. [PubMed: 18284372]
38. Fiala JC, Feinberg M, Peters A, Barbas H. Mitochondrial degeneration in dystrophic neurites of senile plaques may lead to extracellular deposition of fine filaments. Brain Struct Funct. 2007; 212(2):195–207. [PubMed: 17717688]
39. Hering H, Sheng M. Dendritic spines: structure, dynamics and regulation. Nat Rev Neurosci. 2001; 2(12):880–888. [PubMed: 11733795]
40. Pontrello CG, Ethell IM. Accelerators, brakes, and gears of actin dynamics in dendritic spines. Open Neurosci J. 2009; 3:67–86. [PubMed: 20463852]
41. Zhang J, Zhang L, Jiao H, Zhang Q, Zhang D, Lou D, Katz JL, Xu M. c-Fos facilitates the acquisition and extinction of cocaine-induced persistent changes. J Neurosci. 2006; 26(51):13287–13296. [PubMed: 17182779]

42. Bramham CR, Messaoudi E. BDNF function in adult synaptic plasticity: the synaptic consolidation hypothesis. Prog Neurobiol. 2005; 76(2):99–125. [PubMed: 16099088]
43. Tolwani RJ, Buckmaster PS, Varma S, Cosgaya JM, Wu Y, Suri C, Shooter EM. BDNF overexpression increases dendrite complexity in hippocampal dentate gyrus. Neuroscience. 2002; 114(3):795–805. [PubMed: 12220579]
44. Cheung ZH, Chin WH, Chen Y, Ng YP, Ip NY. Cdk5 is involved in BDNF-stimulated dendritic growth in hippocampal neurons. PLoS Biol. 2007; 5(4):e63. [PubMed: 17341134]
45. Ji Y, Lu Y, Yang F, Shen W, Tang TT, Feng L, Duan S, Lu B. Acute and gradual increases in BDNF concentration elicit distinct signaling and functions in neurons. Nat Neurosci. 2010; 13(3): 302–309. [PubMed: 20173744]
46. Danzer SC, Crooks KR, Lo DC, McNamara JO. Increased expression of brain-derived neurotrophic factor induces formation of basal dendrites and axonal branching in dentate granule cells in hippocampal explant cultures. J Neurosci. 2002; 22(22):9754–9763. [PubMed: 12427830]
47. Zhang L, Lou D, Jiao H, Zhang D, Wang X, Xia Y, Zhang J, Xu M. Cocaine-induced intracellular signaling and gene expression are oppositely regulated by the dopamine D1 and D3 receptors. J Neurosci. 2004; 24(13):3344–3354. [PubMed: 15056714]
48. Richtand NM. Behavioral sensitization, alternative splicing, and d3 dopamine receptor-mediated inhibitory function. Neuropsychopharmacology. 2006; 31(11):2368–2375. [PubMed: 16855531]
49. Jiao H, Zhang L, Gao F, Lou D, Zhang J, Xu M. Dopamine D(1) and D(3) receptors oppositely regulate NMDA- and cocaine-induced MAPK signaling via NMDA receptor phosphorylation. J Neurochem. 2007; 103(2):840–848. [PubMed: 17897358]
50. Xu M, Koeltzow TE, Santiago GT, Moratalla R, Cooper DC, Hu XT, White NM, Graybiel AM, White FJ, Tonegawa S. Dopamine D3 receptor mutant mice exhibit increased behavioral sensitivity to concurrent stimulation of D1 and D2 receptors. Neuron. 1997; 19(4):837–848. [PubMed: 9354330]
51. Gao Y, Dickerson JB, Guo F, Zheng J, Zheng Y. Rational design and characterization of a Rac GTPase-specific small molecule inhibitor. Proc Natl Acad Sci U S A. 2004; 101(20):7618–7623. [PubMed: 15128949]
52. Li J, Liu N, Lu K, Zhang L, Gu J, Guo F, An S. Cocaine-induced dendritic remodeling occurs in both D1 and D2 dopamine receptor-expressing neurons in the nucleus accumbens. Neurosci Lett. 2012; 517(2):118–122. [PubMed: 22561554]
53. Xie Z, Srivastava DP, Photowala H, Kai L, Cahill ME, Woolfrey KM, Shum CY, Surmeier DJ, Penzes P. Kalirin-7 controls activity-dependent structural and functional plasticity of dendritic spines. Neuron. 2007; 56(4):640–656. [PubMed: 18031682]
54. Kopec CD, Li B, Wei W, Boehm J, Malinow R. Glutamate receptor exocytosis and spine enlargement during chemically induced long-term potentiation. J Neurosci. 2006; 26(7):2000–2009. [PubMed: 16481433]
55. Missale C, Nash SR, Robinson SW, Jaber M, Caron MG. Dopamine receptors: from structure to function. Physiol Rev. 1998; 78(1):189–225. [PubMed: 9457173]
56. Robinson TE, Kolb B. Structural plasticity associated with exposure to drugs of abuse. Neuropharmacology. 2004; 47(Suppl 1):33–46. [PubMed: 15464124]
57. Hamilton TJ, Wheatley BM, Sinclair DB, Bachmann M, Larkum ME, Colmers WF. Dopamine modulates synaptic plasticity in dendrites of rat and human dentate granule cells. Proc Natl Acad Sci U S A. 2010; 107(42):18185–18190. [PubMed: 20921404]
58. Ren Z, Sun WL, Jiao H, Zhang D, Kong H, Wang X, Xu M. Dopamine D1 and *N*-methyl-d-aspartate receptors and extracellular signal-regulated kinase mediate neuronal morphological changes induced by repeated cocaine administration. Neuroscience. 2010; 168(1):48–60. [PubMed: 20346392]
59. Martin BJ, Naughton BJ, Thirtamara-Rajamani K, Yoon DJ, Han DD, Devries AC, Gu HH. Dopamine transporter inhibition is necessary for cocaine-induced increases in dendritic spine density in the nucleus accumbens. Synapse. 2011; 65(6):490–496. [PubMed: 20936687]
60. Zhang L, Li J, Liu N, Wang B, Gu J, Zhang M, Zhou Z, Jiang Y. Signaling via dopamine D1 and D3 receptors oppositely regulates cocaine-induced structural remodeling of dendrites and spines. Neurosignals. 2012; 20(1):15–34. [PubMed: 22076064]

61. Lin YC, Yeckel MF, Koleske AJ. Abl2/Arg controls dendritic spine and dendrite arbor stability via distinct cytoskeletal control pathways. J Neurosci. 2013; 33(5):1846–1857. [PubMed: 23365224]

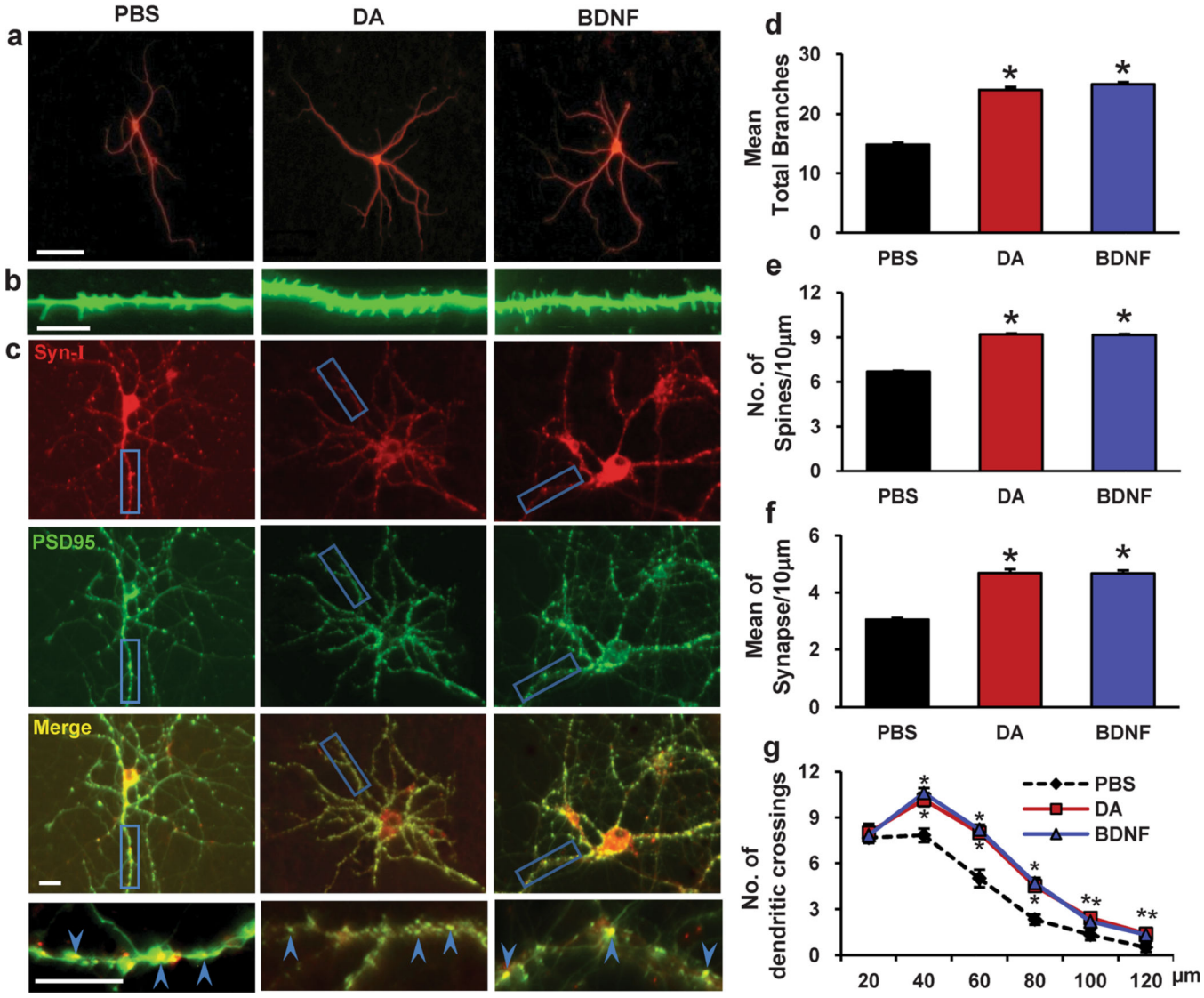

Fig. 1.

Repeated dopamine exposure induces dendritic morphogenesis in PFC neurons. Dopamine was added to the culture medium at 11, 13 and 15 d (1 μM, 30 min). **a** Representative images of MAP2-labeled dendritic branching of PFC neurons. **b** Representative images of γ-actin-labeled spines. **c** Synapsin I is shown in *red*, and PSD-95 is shown in *green*; areas in which they colocalize (*yellow*) indicate the synapse position. **d**, **e**, **f** Quantification of dendritic branching, dendritic spines and synapse number. The data are presented as the mean ± SEM. **p*<0.05 (*n*=2430, ANOVA) vs. PBS-treated PFC neurons. Scale bar, 10 μm. **g** The changes in dendrite complexity of the neurons revealed by Sholl analysis of the intersection number per 20-μm radial unit distance from soma of MSNs. *n*=24–30. **p*<0.05 compared with PBS-treated neurons; $^{\#}p$ <0.05 compared with dopamine-treated neurons

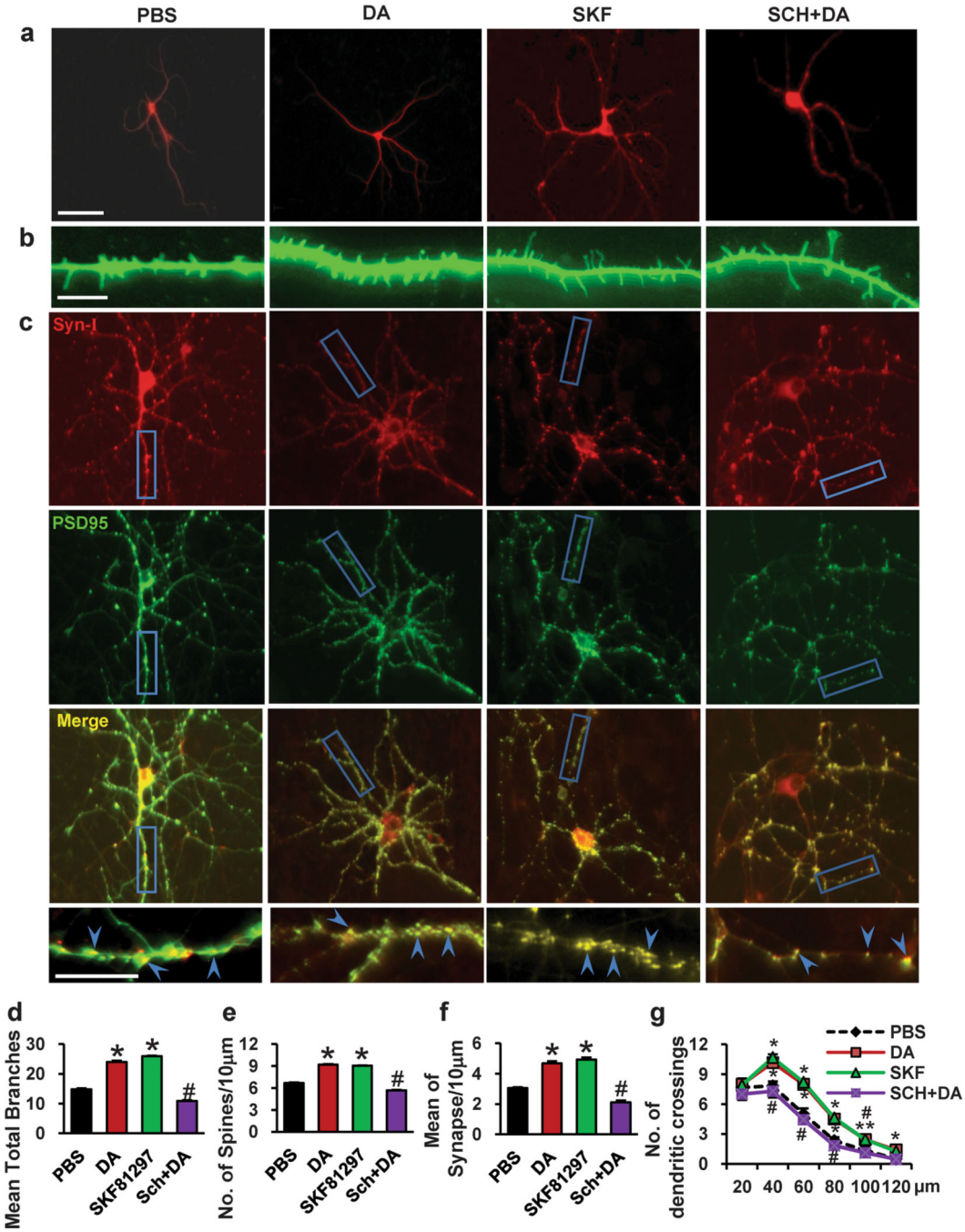

Fig. 2.

The D1 inhibitor SCH23390 inhibited DA-induced neuronal morphogenesis, and the D1 agonist SKF81297 increased neuronal morphogenesis. Neurons were treated with SKF81297 (1 μM, 15 min), or were treated with SCH233990 (10 μM) 5 min before dopamine treatment (1 μM, 30 min) at 11, 13 and 15 d. **a** Representative images of MAP2-labeled dendritic branching of PFC neurons. **b** Representative images of γ-actin-labeled spines. **c** Synapsin I is shown in red, and PSD-95 is shown in green; areas in which they colocalize (yellow) indicate the synapse position. **d**, **e**, **f** Quantification of dendritic

branching, dendritic spines and synapse number. The data are presented as the mean ± SEM. *p<0.05 (n=24–30, ANOVA) vs. PBS-treated PFC neurons. $^{\#}p$<0.05 (n=24–30, ANOVA) vs. the DA treatment group. Scale bar, 10 μm. **g** The changes in dendrite complexity of the neurons revealed by Sholl analysis of the intersection number per 20-μm radial unit distance from soma of MSNs. n=24–30. *p<0.05 compared with PBS-treated neurons; $^{\#}p$<0.05 compared with dopamine-treated neurons

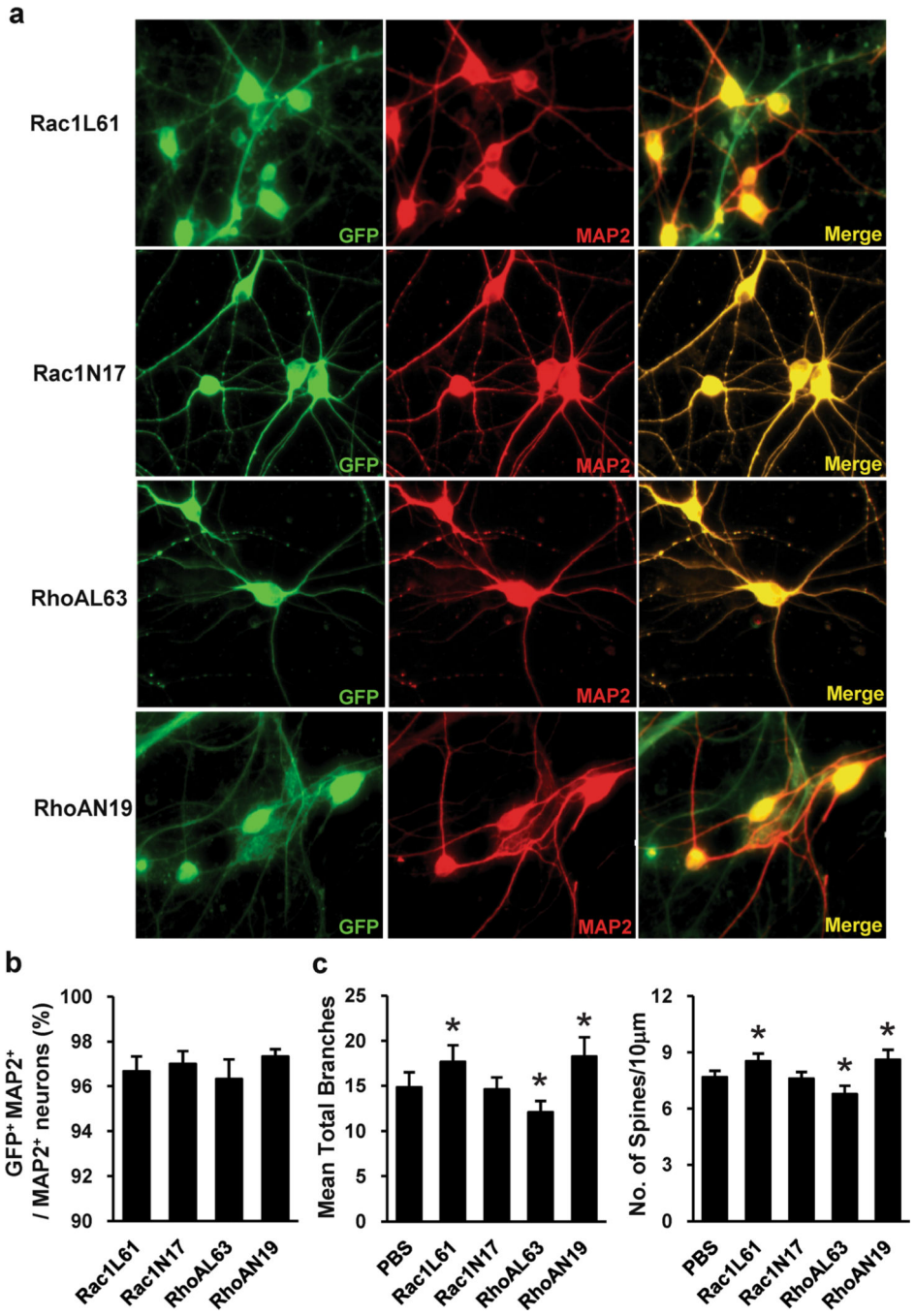

Fig. 3.

Rho GTPase mutant expression in PFC neurons. **a** Representative Images of PFC neurons after Rac1N17 and RhoAN19 lentivirus infection, staining with antibodies against GFP and MAP2. **b** Quantitation of the percentage of GFP-MAP2-double-positive (infected) neurons. The percentage of GFP-MAP2-double-positive neurons was determined by fluorescence microscopy, counting 30 microscopic fields per virus. Recombinant viruses infected >95 % of the neurons. Values are expressed as mean ± SEM. **c** The dendritic branching and

dendritic spine density in PFC neurons expressing Rac1N17, Rac1L61, RhoAN19 or RhoAL63. The data are presented as the mean ± SEM. *p<0.05

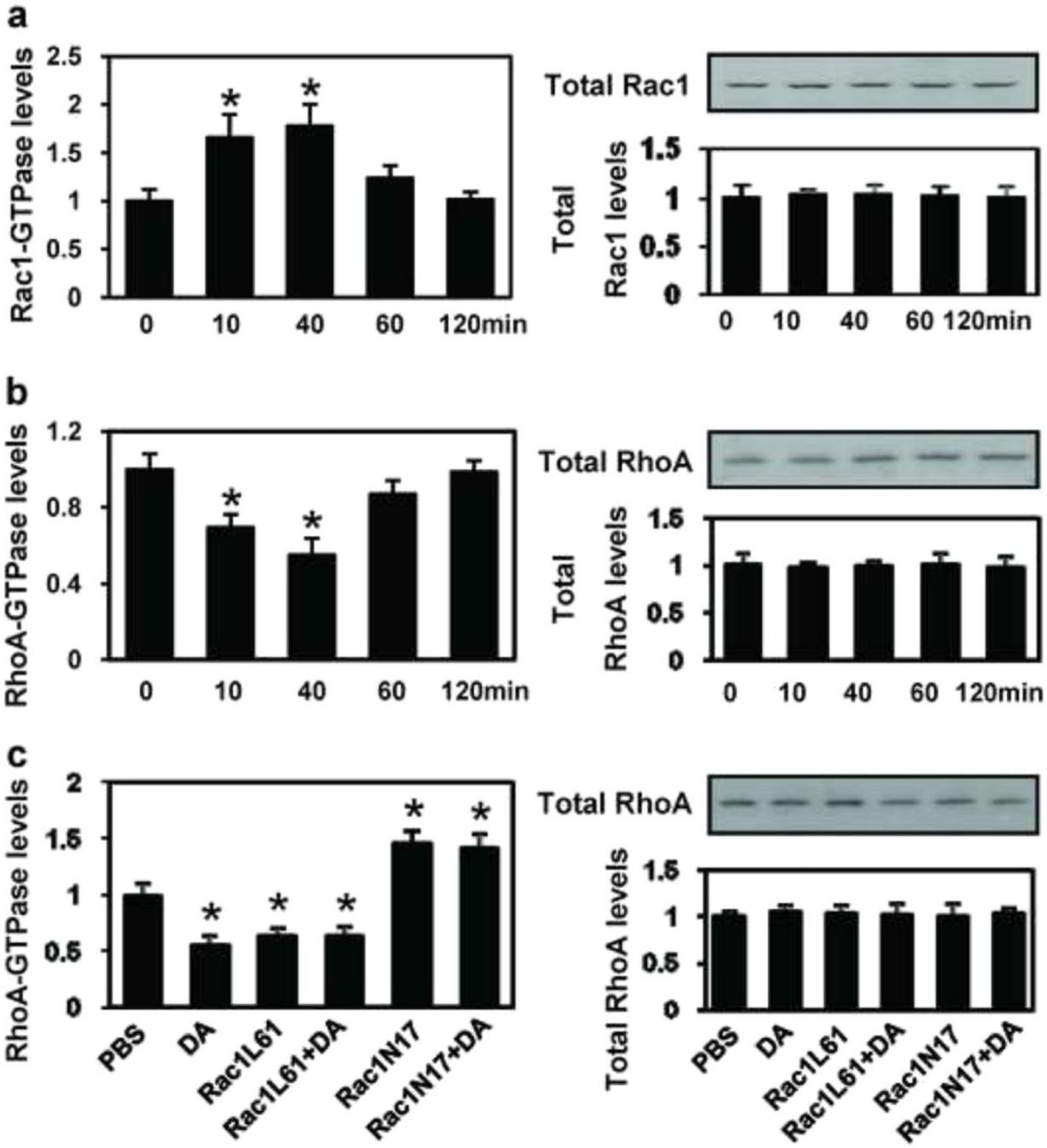

Fig. 4.

Dopamine exposure causes time-course changes in Rac1 and RhoA activity. PFC neurons were plated in 35-mm dishes at a density of 1×10^5 cells/dish treated with dopamine (1 μM) on days 11, 13, and 15 in culture, then lysed and collected at 20, 40, 60 and 120 min (**a** and **b**) or at 40 min (**c**) following the last treatment. The supernatants were used in the G-LISA™ assay. **a** Rac1 activity analysis by G-LISA™ assay at different time points after dopamine exposure. **b** RhoA activity analysis by G-LISA™ assay at different time points

after dopamine exposure. **c** RhoA activity analysis by G-LISA™ assay after different treatment

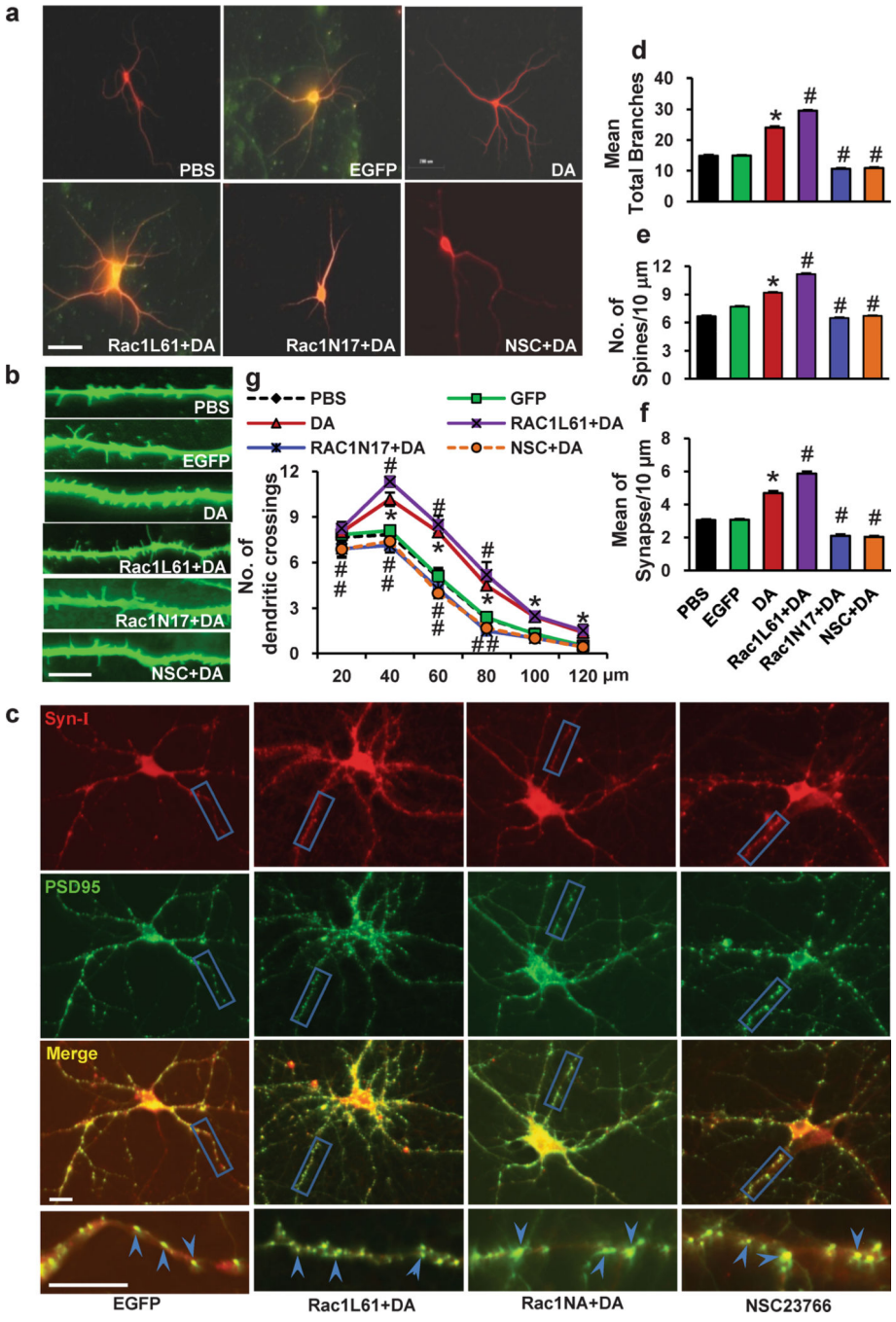

Fig. 5.

Rac1 has a positive role in the dopamine-induced morphological morphogenesis of the PFC neurons. PFC neurons at DIV7 were infected with Rac1N17 or Rac1L61 lentiviruses and treated with either vehicle or DA (1 μM, 30 min) on days 11, 13 and 15 in culture. NSC23766 was selected as a Rac1-specific inhibitor (100 μM, 3 min before dopamine stimulation). **a** Representative images of MAP2-labeled dendritic branching of PFC neurons. **b** Representative images of γ-actin-labeled spines. **c** Synapsin I is shown in red, PSD-95 is shown in green; areas in which they colocalize (yellow) indicate the synapse position. **d**, **e**, **f**

Quantification of dendritic branching, dendritic spines and synapse number. The data are presented as the mean ± SEM. *p<0.05 (n=24–30, ANOVA) vs. PBS-treated PFC neurons. $^{\#}p$<0.05 (n=24–30, ANOVA) vs. the DA treatment group. Scale bar, 10 μm. **g** The changes in dendrite complexity of the neurons revealed by Sholl analysis of the intersection number per 20-μm radial unit distance from soma of MSNs. n=24–30. *p<0.05 compared with PBS-treated neurons; $^{\#}p$<0.05 compared with dopamine-treated neurons

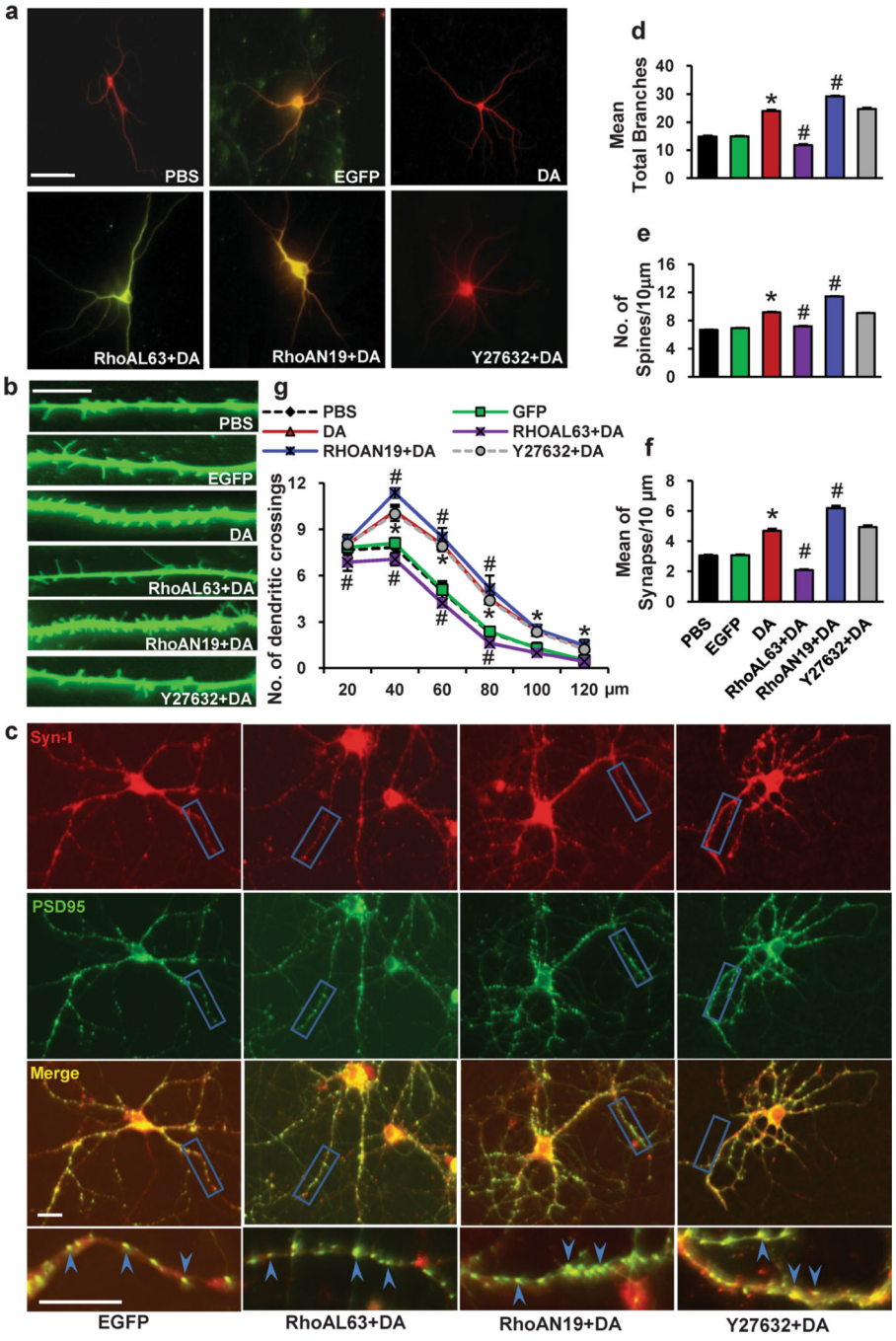

Fig. 6.

RhoA has a negative effect on the dopamine-induced morphological morphogenesis of the PFC neurons. PFC neurons at DIV7 were infected with RhoAN19 or RhoAL63 lentiviruses and treated with either vehicle or DA (1 μM, 30 min) on days 11, 13 and 15 of culture. A specific inhibitor of ROCK (which functions downstream of RhoA), Y27632 (100 μM), was added 3 min before dopamine stimulation. **a** Representative images of MAP2-labeled dendritic branching of PFC neurons. **b** Representative images of γ-actin-labeled spines. **c** Synapsin I is shown in red, and PSD-95 is shown in green areas in which they colocalize

(yellow) indicate the synapse position. **d**, **e**, **f** Quantification of dendritic branching, dendritic spines and synapse number. The data are presented as the mean ± SEM. *p<0.05 (n=24–30, ANOVA) vs. PBS-treated PFC neurons. $^{\#}p$<0.05 (n=24–30, ANOVA) vs. the DA treatment group. Scale bar, 10 μm. **g** The changes in dendrite complexity of the neurons revealed by Sholl analysis of the intersection number per 20-μm radial unit distance from soma of MSNs. n=24–30. *p<0.05 compared with PBS-treated neurons; $^{\#}p$<0.05 compared with dopamine-treated neurons

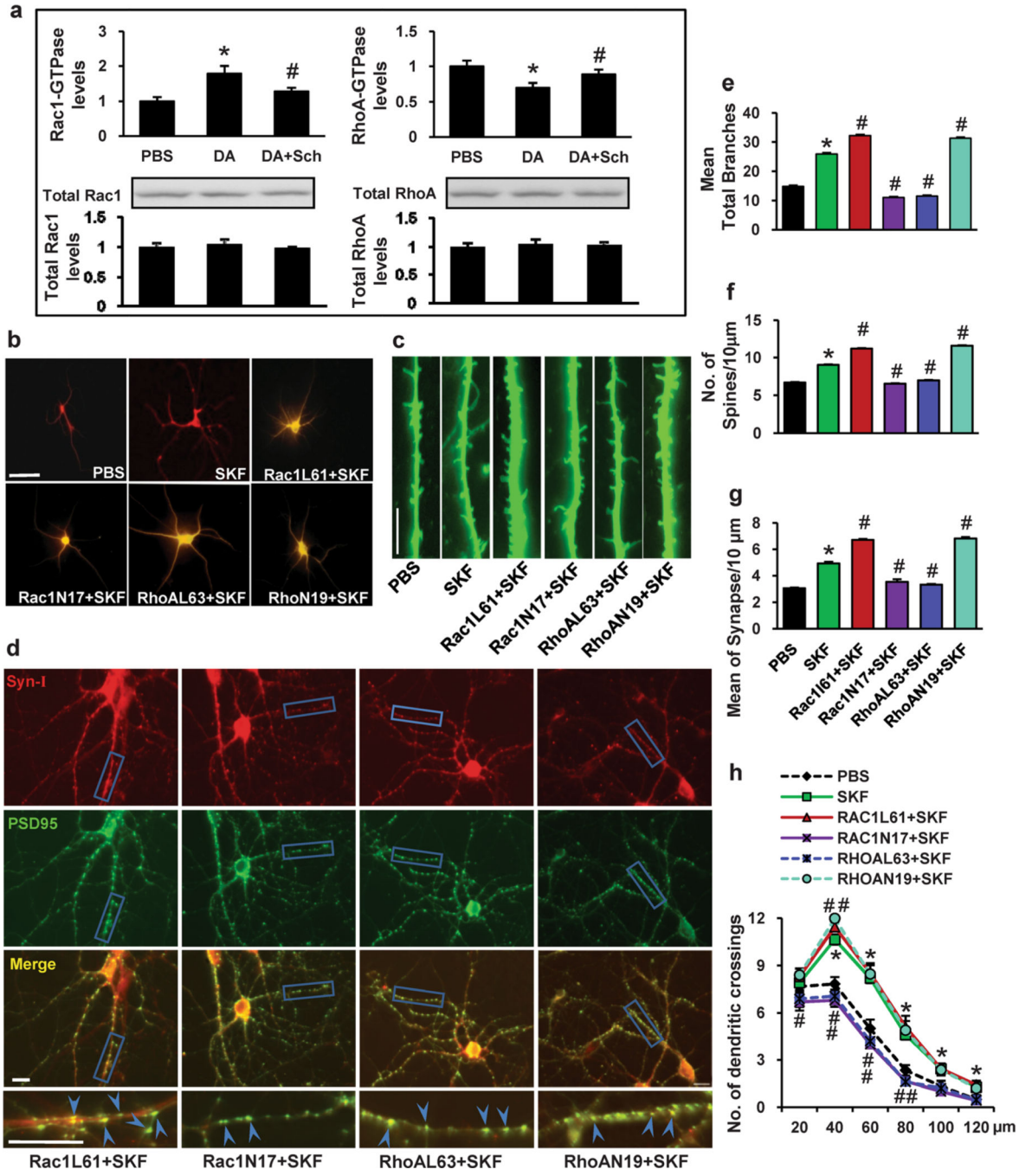

Fig. 7.

The D1 dopamine receptor regulates Rac1 and RhoA GTPase as downstream effectors in DA-induced neuron morphogenesis. PFC neurons were treated with dopamine (1 μM) on days 11, 13, and 15 in culture. **a** Effect of SCH23390 on dopamine-induced Rac1 and RhoA activity at 40 min following the last treatment. **b** Representative images of MAP2-labeled dendritic branching of PFC neurons. **c** Representative images of γ-actin-labeled spines. **d** Synapsin I is shown in red, and PSD-95 is shown in green; areas in which they colocalize (yellow) indicate the synapse position. **e**, **f**, **g** Quantification of dendritic branching, dendritic

spines and synapse number. The data are presented as the mean ± SEM. *p<0.05 (n=24–30, ANOVA) vs. PBS-treated PFC neurons. $^{\#}p$<0.05 (n=24–30, ANOVA) vs. the SKF treatment group. Scale bar, 10 μm. **h** The changes in dendrite complexity of the neurons revealed by Sholl analysis of the intersection number per 20-μm radial unit distance from soma of MSNs. n= 24–30. *p<0.05 compared with PBS-treated neurons; $^{\#}p$<0.05 compared with SKF-treated neurons

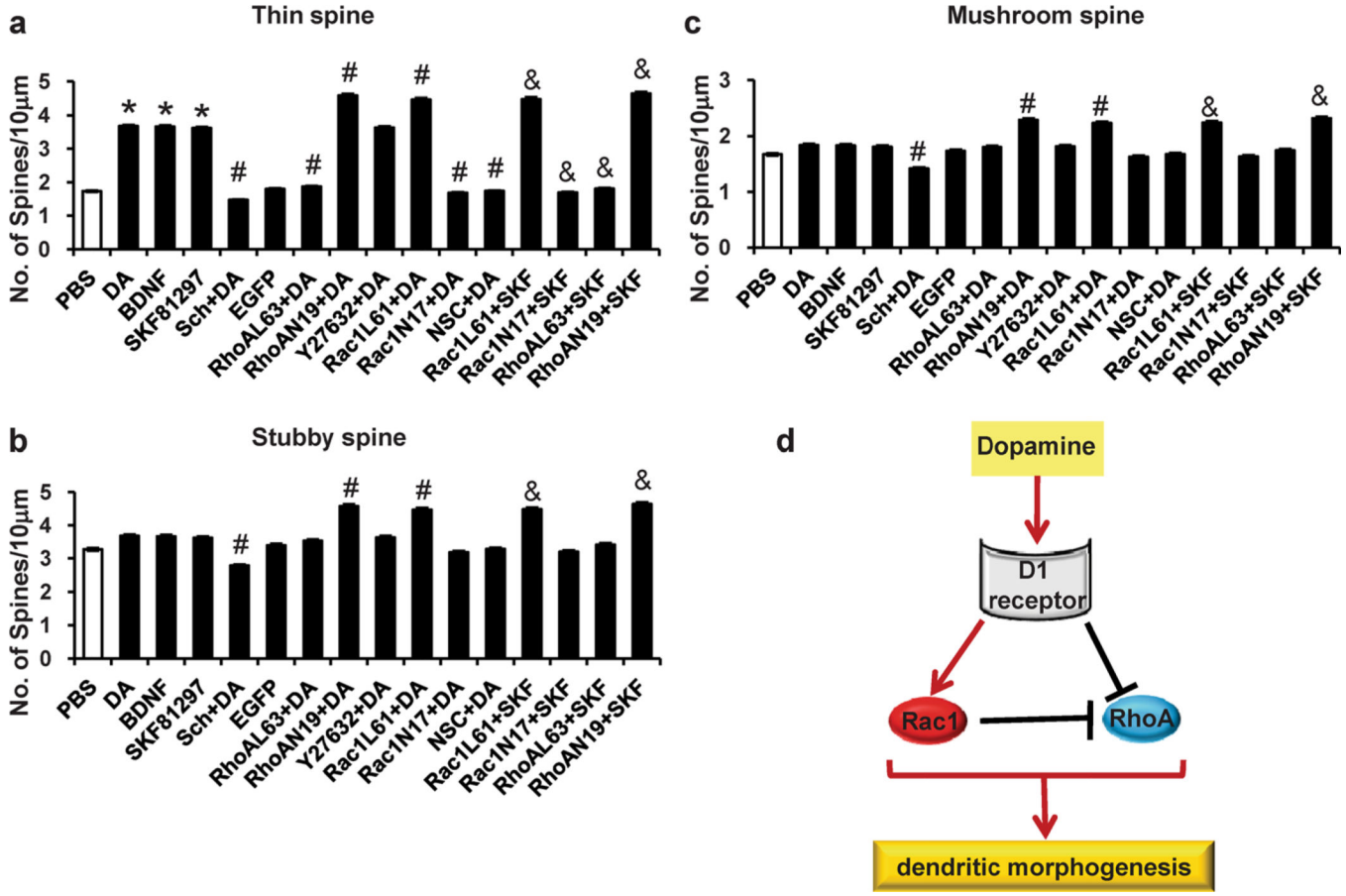

Fig. 8.

The spine type analysis in the dopamine/SKF-induced morphogenesis in the PFC neurons. PFC neurons at DIV7 were infected with Rac1N17/Rac1L61 or RhoAN19/RhoAL63 lentiviruses and treated with either vehicle or DA (1 μM, 30 min) or SKF81297 (1 μM, 15 min) on days 11, 13 and 15 in culture. NSC23766 (100 μM, 3 min before dopamine stimulation), Y27632 (100 μM, 3 min before dopamine stimulation) were used. **a**, **b**, **c** The changes of thin, stubby, and mushroom spine density induced by different treatments in the PFC neurons. **d** Schematic illustration of the experimental model. The data are presented as the mean ± SEM. *$p<0.05$ (n=24–30, ANOVA) vs. PBS-treated PFC neurons. $^{\#}p<0.05$ (n=24–30, ANOVA) vs. the DA treatment group. &$p<0.05$ (n=24–30, ANOVA) vs. the SKF81297 treatment group